620.1123
Ir9f

[redacted]
UNIVERSITY OF ILLINOIS
URBANA, ILLINOIS

T.&A.M. REPORT NO. 202

FRACTURING AND FRACTURE MECHANICS

by

Dr. George R. Irwin

Superintendent, Mechanics Division,
Naval Research Laboratory

DEPARTMENT OF THEORETICAL AND APPLIED MECHANICS
UNIVERSITY OF ILLINOIS

T. & A. M. DEPARTMENT REPORTS:

The Department of Theoretical and Applied Mechanics at the University of Illinois, established in 1890 as a separate unit of the College of Engineering, has the following threefold purpose: (1) to offer instruction in engineering mechanics to undergraduate students, (2) to teach and train graduate students in the field of mechanics, and (3) to conduct a comprehensive research program resulting in the extension of knowledge in all branches of mechanics and related fields. From its inception, the department has offered courses in mechanics in partial fulfillment of the degree requirements of the other departments of the College and, since 1957, the degree of *Bachelor of Science* in Engineering Mechanics has been administered by the department. The granting of graduate degrees originated in 1908, both *Master of Science* and *Doctor of Philosophy* degrees being offered. Research is considered to be a basic part of the educational program; strong emphasis is placed on the fact that the functions of teaching and research go hand in hand for the most complete and effective development of both students and staff.

In general, the research studies are of a fundamental nature that supplement the regular educational functions of the department. They either show the application of the accepted concepts of the engineering sciences to problems in widely divergent fields or produce new concepts with which to attack specialized aspects of problems. Current projects are in the fields of mechanical properties of materials, mechanics of fluids, mechanics of solids, and dynamics. Many of these studies are of a complex analytical nature. However, extensive facilities and unique special equipment are also available for research and advanced study of engineering components which operate under extreme environmental conditions that lead to new problems for which standard design procedures are inadequate. Ten different laboratories are operated with special facilities for studies of concrete, fluid mechanics, fatigue, properties of metals, plastics, vibration, photoelasticity, creep, railroad rails and wheels, and experimental strain measurements employing electronic instrumentation.

The results of research studies conducted in the department are generally disseminated in *T. & A. M. Department Reports*. These present information of an enduring nature, such as the final report of a research contract, and in turn are given a wide initial distribution. After the remainder of the initial printing has been requested and distributed, copies are available on loan (or on purchase in microfilm form)* from the Acquisitions Department of the Library, University of Illinois, Urbana, Illinois. A list of recent reports is included inside the back cover of this report.

For further information
address inquiries to:

T. J. Dolan, Head of the Department
212 Talbot Laboratory
Urbana, Illinois

---

* Charges for microfilm copy are 4¢ per exposure plus mailing cost and 25¢ service charge.

T. & A. M. Report No. 202

[redacted] LIBRARY
UNIVERSITY OF ILLINOIS
URBANA, ILLINOIS

FRACTURING AND FRACTURE MECHANICS

by

Dr. George R. Irwin
Superintendent, Mechanics Division,
Naval Research Laboratory

A Summary of the first of three
Series of lectures delivered
in the

DEPARTMENT OF THEORETICAL AND APPLIED MECHANICS
UNIVERSITY OF ILLINOIS

October 1961

[redacted]

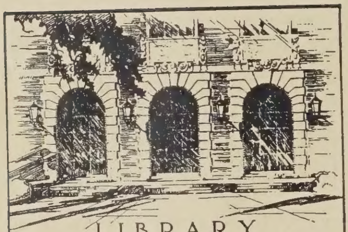

LIBRARY
OF THE
UNIVERSITY
OF ILLINOIS

620.1123
In9f

[redacted]

620.1123
Ir9f

[redacted]

ABSTRACT

Appearance features provide extensive and valuable information about fracturing. Descriptive analysis, one finds, can be based upon a relatively simple model which assumes the crack is a flat internal free surface embedded in a linear elastic stress field. The crack-extension force G corresponding to this model is the Griffith crack theory strain energy release rate. A factor K, proportional to $\sqrt{G}$, represents the stress elevation near the crack border. Crack toughness may be defined as the critical value K_c (or G_c) for onset of rapid crack extension.

A crack traversing a plate converts from the transverse tensile to the oblique shear fracture mode as the size of the crack border plastic strain zone begins to exceed the plate thickness. When fracture mode transition is suppressed by elastic constraint a brittleness temperature of fundamental significance is not observed. For high strength pressure vessels an estimated plastic zone size of twice the platethickness corresponds to a "leak before break" toughness criterion.

For structural metals G_c exceeds solid state surface energy by a factor of the order of 10^4. Apparently lattice slip and the non-coplanor character of crack border elements each provide a hundred-fold increase of crack toughness. In its general aspects fracture strength is dominated by flaws and flaw growth rates.

ACKNOWLEDGEMENT

The content of these 1961 University of Illinois lectures will be used by the author for a monograph entitled "Fracture Mechanics".

The Department of Theoretical and Applied Mechanics gratefully acknowledges the cooperation of the Ford Foundation in providing the funds in its Intramural Faculty Development Program which made it possible to invite Dr. Irwin to present these lectures on our campus in the spring of 1961.

[redacted]

Table of Contents

		Page No.
I	Appearance Features of Fracture	1
II	The Elementary Mathematical Model of Fracture Mechanics	3
III	Crack Toughness Measurements	9
IV	Fracture Mode Transition and Service Toughness Requirements	12
V	Sources of Crack Toughness	16
VI	A Comment on Load Transfer Balance in a Fiber Composite	19

List of Figures

Figure No. Starting on page 23

1 Parabola markings on Plexiglas.

2 Fracture origin showing arrest lines.

3 Fracture originating at the intersection of a keyway.

4 Fracture originating through a similar section but ending at keyway.

- 4-1. Glass rod fracture showing Wollner lines and hackle.
- 4-2. Fracture of a Plexiglas sheet in tension from a cal. 22 bullet perforation, shows multiple branching.

5 Rectangular coordinates, x, y, z, and polar coordinates, r, θ, at the edge of a penny-shaped interior crack.

6 Isochromatic fringes - 4 micro-flash views of the same crack traversing a sheet of Columbia resin (Wells and Post).

7 Central-notch and edge-notch sheet tensile specimens.

8 Schematic curves showing growth of resistance to crack extension, curve R, and three $\mathcal{G}$ versus $\underline{a}$ curves (each for a different fixed tensile load, σ).

9 Width effect in sheets of 7075-T6 aluminum. K_{co} values were computed using no plastic strain correction. Tension was transverse to the rolling direction.

10 K_c versus reciprocal plate thickness 1/B for 7075-T6 aluminum. Tension was parallel to the rolling direction.

11 Fracture appearance for 1/4", 3/16" and 1/8" plates of 7075-T6 aluminum.

12 Percent shear lip as a function of β_c for a variety of heat treatments of various high-strength steels (X, O) and titanium alloys (T). Sheet thicknesses ranged from 0.07 in. to 0.22 in. and all tests were at room temperature.

13 Spreading of part-through crack.

14 Typical test specimens for measurement of weld border and base metal crack toughness.

Digitized by the Internet Archive
in 2024 with funding from
University of Illinois Urbana-Champaign Alternates

https://archive.org/details/fracturingfractu00irwi

List of Figures
(continued)

Figure No.

15 K_{Ic} values from crack-notch tensile tests by Wessel on specimens from a rotor steel forging are shown in the range -- 320° F through 0° F. K_{Ic} values calculated from centrally notched spin disk tests reported by Winne and Wundt for a similar rotor forging are shown in the range 0° F to 400° F.

16 Sketch by Leonardo da Vinci of his apparatus for testing iron wire.

17 Logarithm of average tensile strength (psi) as a function of logarithm of specimen length (cm) for carefully protected glass fibers (x) and fibers damaged by rough handling (o).

I. Appearance Features of Fracture

The extension of a crack is a locally discontinuous process. In the overstressed zone ahead of the main crack local inequalities of strength cause non-uniform patterns of plastic strain. New openings are formed in regions of greatest tensile weakness. The extension and joining of these with neighboring openings and with the main crack constitute the complex process of crack extension. Figure 1 shows parabola-shaped markings on a fracture of Plexiglas. The arms of the parabolas open out in the direction of crack propagation. The new openings ahead of the main crack are not coplanar. Thus, as the outward spread of the crack from a new origin is overtaken by the main crack, the level difference is progressively broken through. In this way curved tear lines are formed whose appearance suggests a parabola although no exact correspondence to that mathematical contour actually exists.

The extension of tear lines from new initiation points is a prominent feature of fracture appearance. This feature is used to trace the direction of crack propagation and thus to permit determination of the region from which crack propagation developed.

When the leading edge of a crack extends after an arrest period due to unloading, the alignment of new initiation points along the arrest position is indicated by new tear lines as shown on Figure 2. The starting crack attained final critical size relative to fast propagation during three loading cycles.

Except for local irregularities a tensile crack traversing a plate follows a path normal to the direction of maximum tensile stress. Similarly a flat tensile crack severing a thick section follows a locus plane normal to the maximum tensile stress. As such a crack approaches a free surface the greatest tension is parallel to the free surface and so the approach to the free surface is at right angles. However, as the unsevered section becomes relatively small the reduction of constraint coupled with stress elevation results in rapid development of large plastic strains. Due to these plastic strains the character of the final breakthrough to the free surface usually takes the form of an oblique shear separation. Figure 3 shows a fracture originating at the intersection of a keyway with the snap ring groove of the aft snap ring boss on a rocket engine chamber of out-moded design. Figure 4 shows a fracture through a similar section of another chamber in which the fracture markings clearly indicate the opposite direction of crack propagation. Note in Figure 4 that the snap ring groove is completely framed by a lip of oblique shear fracture.

If a common glass stirring rod is file-notched and broken with a quick bending motion, a fracture appearance like that shown by Figure 4-1 is obtained. The intersecting families of lines curving across the fracture surface are called Wollner lines and are formed in the following way. The locus of the leading edge of the crack running from the surface notch origin is nearly a section of a circle. In the mirror portion of the fracture evidence for discontinuous fracturing is on too small a scale to be observable. However, irregularities or discontinuities in progressive separation do occur where the leading edge of the crack intersects the free surfaces. These cause elastic wave vibrations and the responsive tilt of the fracture surface traces out lines where each large vibration contacted the leading edge of the crack. From the intersection angles and knowledge of the elastic wave velocity it is possible to obtain rather accurately the velocity of the leading edge of the crack. Evidence thus obtained, largely by Shardin and Kirkhof (Freiburg), shows the velocity increases rapidly at first then levels off at a value about half the velocity of an elastic shear wave. Simultaneous with attainment of limiting speed a roughening of the fracture surface appears, called "hackle". Hackle results from the joining of overlapping fracture surfaces accompanied by formation of free slivers of glass called "shards". As the crack approaches the side of the rod which was originally in compression, the velocity drops and the fracture surface again becomes smooth.

A similar phenomenon relative to limiting velocity occurs in the run of a through-the-thickness crack traversing a plate as illustrated by Figure 4-2. This figure shows the development of branching in a plate of plexiglas. Velocity measurements from high speed motion pictures indicated a limiting velocity was reached coincident with the beginning of crack division.

Table I shows limiting crack velocities for various materials in comparison to half the shear wave velocity. The reason for this particular limit is somewhat obscure. Nevertheless, it is clear enough that crack extension is always slow relative to elastic wave velocities. Virtually the entire elastic energy driving force converts to heat energy as the crack moves. The velocity remains in phase with the driving force and never attains more than half the speed of the slowest of the principal elastic wave velocities. When the driving force exceeds the amount necessary for the limiting crack speed, the crack simply divides and the segments move no faster.

Fracture appearance features are so sensitive to circumstances relative to an understanding of the process that they well repay careful study. For example, in the solution of existing fracture problems fracture examinations are of primary importance. Fracture appearance features indicate where the primary crack opening developed and the subsequent run and branching events which produced the final fractured condition. The amount of oblique shear fracture gives a rough indication of the toughness of the material. The presence and degree of general yielding near the primary origin crack suggests the general level of stress governing starting crack development. Since fracture origins develop at regions of greatest tensile weakness a flaw of some nature can usually be discerned at the origin of the starting crack. A study of the nature of this flaw, assisted as appropriate by metallographic examinations, is always of interest. The path of the running crack frequently reveals secondary fracture origins of sufficient prominence to deserve study and consideration. Auxiliary analytical studies to provide better estimates of stresses near the starting crack are helpful. A complete descriptive picture of the fracture event consistent with all known facts provides a sound basis for discussion of remedies.

Three principal factors influence service fracture failures. These are:

1. Stress level abnormally high;
2. A flawed condition or prior crack of unusual severity;
3. An unexpectedly low degree of crack toughness.

The character of the remedy appropriate to a given situation differs depending upon how the responsibility for failure is assigned relatively among these factors. To assist this determination it is desirable to have a concept of crack toughness closely related to starting crack size and stress level.

II. The Elementary Mathematical Model of Fracture Mechanics

From numerous examinations of structure failures due to fracture one concludes the following behavior pattern is typical. When the starting crack size is very small, say a few hundredths of an inch, the stress supported by the section prior to fracture is invariably equal to or greater than the yield stress. Sections which support only a fraction of the yield stress at failure always contain starting cracks of substantial size.

Our primary aim is to describe, understand, and control the conditions which cause fractures at stresses below the yield stress of the material. We note that in this region of primary interest the stress level is too low to cause general yielding of the section and, secondly, the starting crack is of substantial size. This suggests the basic mathematical model should, at first, neglect the influence of plastic strains and should regard the crack simply as an interior free surface in an elastic solid. Our model choice is also influenced by the fact that the events at the leading edge of the crack are complex. A careful allowance for the influence upon the stress field of plastic strains and advance initiations is not practical. We cannot do it with enough accuracy so that the pay-off is worth the effort. Later it will be seen that a crude adjustment for inelastic strains at the edge of the crack is possible and can be helpfully employed.

Next we examine what is implied by the suggested mathematical model and what can be done with it.

In its general aspects the leading edge of a crack will be represented mathematically as a smooth though possible curved line, shown in Figure 5 as a section of a circle of radius a. Although in later equations we may, for convenience shift the origin of the x, y, z coordinate system the y-direction is always perpendicular to the crack and the x-direction is always the line of expected crack extension. The coordinates, r, θ are used only at the leading edge in the x, y plane as shown here.

When we discuss extension of a through-crack in a sheet the treatment assumes all stresses and strains averaged through the thickness (z-direction) as is customary for generalized plane stress.

Figure 6 shows the isochromatic fringes near a running crack traversing a plate of Columbia resin. The loop pattern designates the elevated stress zone and the spread of this pattern is proportional to the square of the stress elevation factor. The stresses near the leading edge have been measured in terms of fringe orders and distances in experiments of this kind. The crack extension process in all its complexities is confined to a small region from which the isochromatic loops emerge. In order to state the stress environment which surrounds and controls this process we need to determine only the relatively simple stress pattern which pertains to the region close to the leading edge of the crack.

A complete study of the stress analysis methods applicable to crack stress fields would be a whole series of lectures. The remarks here must be brief and somewhat incomplete. Applicable mathematical procedures have been set forth by Neuber, Muskhelishvili, Green, Sneddon, and Westergaard. For two-dimensional problems the Westergaard procedure which will be described is possibly the simplest.

As in most such methods potential functions are used. A potential function is any solution of the LaPlace differential equation and can always be represented as the real or the imaginary part of a function, say Z, of the complex variable, $x + iy$. These are written as $\mathrm{Re}Z$ and $\mathrm{Im}Z$ respectively. With respect to derivatives Westergaard (1) used an odd notation. Z' is the derivative of Z. Z is the derivative of $\bar{Z}$ and $\bar{Z}$ is the derivative of $\bar{\bar{Z}}$.

Assuming the Airy stress function has the form

$$F = \mathrm{Re}\bar{\bar{Z}} + y\,\mathrm{Im}\,\bar{Z} \tag{1}$$

the stresses are given by

$$\sigma_y = \frac{\partial^2 F}{\partial x^2} = \mathrm{Re}Z + y\,\mathrm{Im}\,Z' \tag{2}$$

$$\sigma_x = \frac{\partial^2 F}{\partial y^2} = \mathrm{Re}Z - y\,\mathrm{Im}\,Z' \tag{3}$$

$$\tau_{xy} = -\frac{\partial^2 F}{\partial x\,\partial y} = -y\,\mathrm{Re}Z' \tag{4}$$

For plane strain problems

$$\sigma_z = \nu(\sigma_x + \sigma_y) \tag{5}$$

Now the idea of the Westergaard procedure is to solve a specific problem by an appropriate choice of the stress function Z. For example, the choice

$$Z(\zeta) = \frac{K}{\sqrt{2\pi\,\zeta}} \tag{6}$$

where

$$\zeta = x + iy \tag{7}$$

solves the problem of the stress pattern represented by the region of isochromatic loops near the crack in Figure 6.

Mechanics is the reaction of bodies to forces. Correspondingly in fracture mechanics the force concept is of central importance. For the mathematical model we are using, the appropriate force concept is the rate of loss of strain energy with crack extension, the same energy loss rate which was basic to the Griffith crack theory (2). For the stress field corresponding to the preceding equations the crack extension force is (3)

$$\mathcal{G}_I = \frac{K^2}{E}(1 - \nu^2) \quad - - - - - - - - - - - - - - - - \quad (8)$$

where E is Young's Modulus and ν is Poisson's ratio. The subscript I indicates that the force $\mathcal{G}$ pertains to a stress system which pulls the crack walls directly apart, the opening mode of crack extension.

There are, conceptually, two sliding modes of fracture (4) for which the force values are written as $\mathcal{G}_{II}$, for the forward-sliding mode, and $\mathcal{G}_{III}$, for the parallel-sliding mode. These correspond directionally to the edge and screw type crystalline dislocations. For a crack traversing a plate we discuss crack extension in terms of the average effective crack-extension force for the whole crack, taking no account mathematically of the fact that the fracture is, say, of the opening mode type in central regions and principally in the sliding modes near the free surfaces. The convention used is to designate the total effective crack-extension force by the symbol $\mathcal{G}$ with no Roman numeral subscript. For simplicity we consider that the $\mathcal{G}$ value for mixed mode fractures always corresponds to generalized plane stress. Calculation of the strain energy release rate, as shown in reference (3), then gives the result,

$$\mathcal{G} = \frac{K^2}{E} \quad - \quad (9)$$

Substituting the stress function of equation (6) into equations (2), (3), and (4) gives

$$\sigma_y = \frac{K}{\sqrt{2\pi r}} \cos\frac{\theta}{2}\left(1 + \sin\frac{\theta}{2}\sin\frac{3\theta}{2}\right) \quad - - - - - - - \quad (10)$$

$$\sigma_x = \frac{K}{\sqrt{2\pi r}} \cos\frac{\theta}{2}\left(1 - \sin\frac{\theta}{2}\sin\frac{3\theta}{2}\right) - \sigma_{ox} \quad - - - - - \quad (11)$$

$$\tau_{xy} = \frac{K}{\sqrt{2\pi r}} \sin\frac{\theta}{2}\cos\frac{\theta}{2}\cos\frac{3\theta}{2} \quad - - - - - - - - - - - \quad (12)$$

In these equations the influences of applied loads and geometry contribute to the crack-edge stress pattern only through two stress field parameters. One of these is K which represents $\sqrt{E\mathcal{G}}$. The other is the uniform stress σ_{ox} directed parallel to the crack surface which can be altered without changing the free boundary conditions along the crack surfaces. The important parameter is K. From observations one finds the speed of crack extension is quite sensitive to the value of K (or the value of $\mathcal{G}$) but is relatively insensitive to σ_{ox}. From the mechanics viewpoint the central problem is to establish significant relationships between crack movement and the values of K or $\mathcal{G}$. As one might intuitively guess the degree of elastic constraint is also important. This is discussed later.

In order to perform and analyze experiments we must be able to determine values of K (or $\mathcal{G}$) for various loads, crack lengths, and geometries. This can be done with the assistance of experimental or theoretical stress analysis. As an example of the theoretical approach consider the stress function

$$Z(\xi) = \sigma\left(1 - \left(\frac{a}{\xi}\right)^2\right)^{-1/2} \qquad (13)$$

This stress function represents a central crack of length 2a in an infinite place with uniform tension σ acting in the y-direction remote from the crack. Along the line of expected crack extension

$$\sigma_y = \sigma\left[1 - \left(\frac{a}{x}\right)^2\right]^{-1/2} \qquad (14)$$

for $x = a + r$ and $r \qquad o$

$$\sigma_y = \sigma\,\frac{(a + r)}{\sqrt{r\,(2a + r)}} \qquad (15)$$

By comparison with equation (10)

$$K = \text{Lim}\ \sqrt{2\pi r}\ \sigma_y \qquad (16)$$

as
$r \longrightarrow o$

Thus we find

$$K = \sigma \sqrt{\pi a} \tag{17}$$

$$\mathcal{G} = \frac{\pi \sigma^2 a}{E} \tag{18}$$

A. A. Griffith was aware of the above value for strain energy release rate from a stress analysis due to Inglis. Assuming $\mathcal{G}$ equal to twice the surface tension he was able to represent approximately the influence of small cracks on the fracture strength of glass. However, as will be explained later, resistance to crack extension is much too complex to permit reliable estimates on this basis even for glass.

A useful variation of the stress function of equation (13) is

$$Z(\xi) = \left\{ 1 - \left(\frac{\sin \frac{\pi a}{W}}{\sin \frac{\pi \xi}{W}} \right)^2 \right\}^{-1/2} \tag{19}$$

Here the position variable ξ is expressed in such a way that the whole stress pattern is periodic across successive strips of width W in the x-direction. The above stress function represents an infinite periodic sequence of cracks of length 2a along the x-axis. The shear stress τ_{xy} is zero along y-direction lines of symmetry, those through the crack centers and those bisecting segments between cracks. To represent a central crack in a tensile strip of finite width two y-direction lines bisecting segments between cracks may be selected as the side boundaries. The model then differs somewhat from the real situation because a distribution of normal forces on the side boundaries exists which should be removed. However, these forces are directed parallel to the crack and their removal has only a small effect on the values of K and $\mathcal{G}$. In a similar way we obtain an approximate representation of a tensile strip having a pair of edge cracks of equal depth, a. In this case y-direction lines through the crack centers serve as side boundaries. In either case use of equation (16) leads to

$$K^2 = \sigma^2 W \tan \frac{\pi a}{W} \tag{20}$$

Figure 7 shows two standard types of sheet tensile specimens either of which may be used for a measurement of crack toughness.

The resistance of a material to crack extension is the dissipation of energy in inelastic strains which opposes the applied crack-extension force. In the modifications of the Griffith theory suggested by Irwin and by Orowan it was implied this resistance could be assumed constant but observations do not substantiate this assumption. The resistance to crack extension measures the total energy dissipation from inelastic straining within the crack extension process zone. With certain reservations for strain rate effects this zone expands with the stress elevation, that is, with the $\mathcal{G}$ value. Thus, normally, the crack-extension resistance increases steadily with crack extension force. We omit discussion of abnormal behavior due to strain rate sensitivity for three reasons: (1) for commercial steels of highest strength (rocket chamber steels) and for high strength aluminum alloys, strain rate sensitivity is relatively small, (2) in other instances the influence of strain rate upon flow stress and fracture is of minor importance, and (3) for clarity, we should consider the least complex patterns of behavior first.

III. Crack Toughness Measurements

Since the resistance to crack extension is not constant we ask next whether there are special values of the resistance which are of sufficient significance to deserve primary attention. Observationally there are only two relatively abrupt process change points. One is the change from slow to fast crack extension in which the crack speed increases several orders of magnitude during only a few percent change in the the value of $\mathcal{G}$. The other is the point of onset of forking in a sheet or hackle in a thick section when the average crack speed reaches a critical value. In structural fracture failures we are concerned more with "whether and why they break" than with "number of fragments". Therefore we give first attention to crack toughness evaluation based upon the resistance to onset of rapid crack propagation.

From comparison of onset of general yielding to onset of general fracturing one can see that measurement of the critical force for the change from slow to fast crack extension is like measurement of yield strength in various ways. In both types of measurement certain arbitrary conventions of testing method are advisable so that results obtained in different laboratories can be compared.

The specimens of Figure 7 were recommended in an ASTM committee report published* in January 1960. A typical specimen might be in the range of 1.5 to 3.0 inches in width and possess other dimensions in proportion as shown on the figure.

---

* ASTM Bulletin, January, 1960.

The ends of the notch are intended to represent actual cracks. A root radius of 0.001 inches does this well enough for metals of moderate toughness but not well enough for some very brittle materials. In order to be sure that the initial slots act like actual cracks it is helpful to initiate fatigue cracks at the notches. Reverse bending is probably the simplest procedure. The fatigue cracks thus started extend across the notch corners. In the tensile test, at a relatively small load, these corner cracks join forming an initial crack of normal shape. With additional increase of tension slow crack growth occurs as indicated on Figure 7. From the tension and crack length at onset of rapid fracture the critical values K_c (or $\mathcal{G}_c$) can be calculated using procedures of theoretical stress analysis.

Normally the maximum load serves well enough as the critical tensile load measurement. The other measurement needed is the crack length at onset of rapid crack extension. Currently use of ink staining is recommended. Either India ink or a staining fluid of similar viscosity is daubed into the notches. With some precautions to prevent splashing and post-fracture creeping of the ink, the ink follows and stains just the slow part of crack extension. For central crack specimens the recommended stress analysis provides the equations

$$K = \sigma \sqrt{W \quad q_o} \qquad \text{- - - - - - - - - - - - - - - - - - -} \qquad (21)$$

$$q_o = \tan u \qquad \text{- -} \qquad (22)$$

$$u = \frac{\pi}{W}\left(a + \frac{K^2}{2\pi\,\sigma^2_{YS}} \right) \qquad \text{- - - - - - - - - - - - - - -} \qquad (23)$$

From these equations

$$\tan^{-1} q_o = \frac{\pi a}{W} + \frac{1}{2}\, q_o \left(\frac{\sigma}{\sigma_{YS}}\right)^2 \qquad \text{- - - - - - - - - - -} \qquad (24)$$

which can be solved graphically for q_o when a/W and σ/σ_{YS} are given.

If equations (21), (22), and (23) are compared with equation (20), one notes that the crack length appearing in the argument of the target function has been increased by the amount

$$a' = \frac{1}{2\pi}\left(\frac{K}{\sigma_{YS}}\right)^2 \qquad \text{- - - - - - - - - - - - - - - -} \qquad (25)$$

The symbol σ_{YS} is intended to represent the resistance of the material to plastic yielding and is, for definiteness, taken to be the 0.2% offset uniaxial tensile yield stress. The term a' is a correction to the stress analysis for local yielding near the crack. In the procedure followed here one must express the stress elevation near the crack extension process zone in terms of a single number K. The one-parameter degree of simplification permits only a limited kind of allowance for plastic flow. Essentially the influence of stress relaxation by local plastic flow upon the surrounding stresses is assumed equivalent to stress relaxation from an additional increment of crack length. From dimensional considerations the size of the plastic zone and the crack length correction are proportional to the length factor, $(K/\sigma_{YS})^2$. If one assumes the net section stress, as conditions of general yielding are approached, would approach the value $1.15\,\sigma_{YS}$ then the crack length correction has the value shown in equation (25).

The stress analysis recommended for use with edge-notched specimens contains, in addition, to the correction for local plastic yielding, an adjustment for the influence of free surface conditions along the side boundaries. The equations for computation of K are

$$K = \sigma \sqrt{W q_2} \quad \text{- - - - - - - - - - - - - - - - - - -} \quad (26)$$

$$q_2 = \tan u + 0.1 \sin 2u \quad \text{- - - - - - - - - - - - - -} \quad (27)$$

and u is given by equation (23).

Use of the plastic zone crack length correction removes from results a substantial portion of a trend with specimen size which would otherwise be present tending to give values of K_c which increase with the size of the test specimen. Contributing to this trend, however, is another effect quite different in nature from the influence of local plastic yielding.

Figure 8 shows schematically a relationship fundamental to onset of fast fracture in crack toughness testing. The crack-extension resistance R shown in the figure is based on consistency considerations, not actual measurements. It is assumed that measurements of the resistance for a fixed speed of crack extension, say 10 inches per second, can be represented by a curve rising and leveling off as shown in the figure. The initial crack extension starting from a very sharp notch or a fatigue crack does not possess a plastic zone of typical size. Thus expansion of the plastic zone and increase of R accompanies the first increments of crack extension. Eventually R must become

UNIVERSITY OF
LIBR

constant for consistency with a fixed crack extension speed. The curved lines represent the relation of the force $\mathcal{G}$ to crack length for a finite width test plate. Each curve is for a different fixed load. After a small crack extension the $\mathcal{G}$ value acting is the intersection of curve A with R. To obtain more crack extension one must increase the load until this intersection finally becomes a tangency as shown by curve B. In a very stiff testing arrangement it is possible to observe continued crack extension with dropping load as illustrated by the intersection of R with curve C. However, in normal testing such a load drop is not observed and onset of rapid fracture appears to coincide with maximum load. The point of tangency occurs below the horizontal asymptote of curve R. The tangency point should occur at larger values of R and $\mathcal{G}$ with increase of specimen size and a trend of K_c with specimen size remains due to this in typical measurements as illustrated by Figure 9. This trend could be eliminated more or less successfully, depending upon plastic flow properties by choosing a larger plastic zone correction factor. However, it seems unwise to eliminate a trend due to one cause by overcorrecting for a second and different effect. In any case the effect of this trend upon results is small compared to the differences generally looked for in fracture testing.

To review crack toughness testing the important elements are as follows: The crack edge stress field has a characteristic pattern. Limiting attention to cracks pulled directly open by tensile forces the major influence of the stress field can be given a one-parameter representation. It is convenient to study crack extension in laboratory tests in terms of this parameter which can be expressed alternatively as the crack-extension force $\mathcal{G}$ or as the stress intensity factor K. A natural selection for standard measurement of crack toughness is the K value K_c for onset of rapid fracture. Any specimen shape might conceptually be used for this measurement granting a stress analysis appropriate for K value calculation was applicable and bearing in mind also the moderate dimensional size effect illustrated in the last slide. In the same terms these laboratory K_c values can be used for a service component containing a crack. In this way our measurement and analysis procedure establish a relationship between stress level, crack size, and crack toughness applicable to real structures.

IV. Fracture Mode Transition and Service Toughness Requirements

Consider next the influence upon crack toughness of elastic constraint. Shown on Figure 10 are measurements of K_c for 7075-T6 aluminum plotted against the reciprocal sheet thickness 1/B. For plates 3/8" or larger in thickness the values of

K_c were measured with a notch-bend testing procedure. A still higher degree of elastic constraint can be obtained with circumferentially-notched bars. Several values from tests of this nature are shown on the ordinate axis and are properly termed K_{Ic} values since they correspond purely to opening mode plain strain crack extension.

Assume, for the moment, that the plastic zone size can be estimated as just twice the plasticity correction factor, or as $(1/\pi)(K_c/\sigma_{YS})^2$. In these terms the dashed line corresponds to a plastic zone size equal to 3/4 of the sheet thickness. Beyond a plastic zone size which is ten times the sheet thickness the measured K_c values begin to decrease. The decrease to the right is understandable but it is not of primary interest here. The region in which the fracture changes from flat tensile to oblique shear with rapidly increasing toughness is the region close to the intersection of the dashed line with the curve through the measurements. Notice that a 1/4" thickness falls below the dashed line while 3/16" and 1/8" thickness are above. Figure 11 shows the fracture appearances for these three thicknesses. When the plastic zone is less than twice the sheet thickness it is still possible for the shear lips to develop independently.

Due to the importance in fracture mode transition of the relative plastic zone size it is convenient to write

$$\beta_c = \frac{1}{B}\left(\frac{K_c}{\sigma_{YS}}\right)^2 \quad \text{- - - - - - - - - - - - - - - -} \quad (28)$$

and

$$\beta_{Ic} = \frac{1}{B}\left(\frac{K_{Ic}}{\sigma_{YS}}\right)^2 \quad \text{- - - - - - - - - - - - - - -} \quad (29)$$

The plastic zone size is roughly one-third of $B\beta_c$. Figure 12 shows fracture appearance in terms of percent shear for a large number of high strength steels and several Ti alloys indicated by T. The abscissa is β_c. Note that beyond a β_c value of 2π (or six) the transition to oblique shear fracture is nearly complete. As will be explained presently a rational basis exists for using the rule $\beta_c = 2\pi$ as a minimum toughness standard for high strength metallic pressure vessels.

Reviewing briefly, it is evident that fracture mode transition can be regarded as a mechanical effect controlled by the relative plastic zone size. Essentially, conditions of plane strain must exist at the leading edge of a flat tensile crack. This is readily provided in central regions of the plate by making the plate thickness large relative to the plastic zone size. At the side free surfaces where thickness direction stress relaxation must occur there is always an oblique shear border. The relative size of the shear border increases with degree of thickness direction stress relaxation. When the plastic zone size is several times the plate thickness the transition to oblique shear is virtually complete. The abruptness of this change is assisted by the large increase in maximum shear stress induced by thickness direction stress relaxation and the corresponding shift from plane strain to plane stress conditions.

The topic considered next is a minimum toughness criterion for pressure vessels built using high strength steel, aluminum, or titanium alloys. Flaws in the nature of through-cracks are not expected. Although the pressure vessel may not be perfect we assume it does not leak. From examination of fracture failures one finds these happenings always develop from the deepening and spreading of a part-through crack as illustrated in Figure 13. If inspection is good and such part-through cracks as exist do not have lengths greater than the plate thickness then the development of a through crack of about twice the plate thickness in effective length must precede general crack propagation. In the initial stages of crack growth pictured here elastic constraint prevents any plastic contraction parallel to the leading edge. This means a relatively low resistance to crack growth. In later stages shear lips form and the governing toughness is the K_c value measured as previously discussed. The equation for K^2 for a through crack of half length $\underline{a}$ is

$$K^2 = \frac{\pi \sigma^2 a}{1 - \frac{1}{2}\left(\frac{\sigma}{\sigma_{YS}}\right)^2} \text{ . - - - - - - - - - - - - - - (30)}$$

Assuming the K value is the critical value K_c, that $\sigma = \sigma_{YS}$, and that $a = B$, one finds

$$K_c^2 = 2\pi \sigma_{YS}^2 B \text{ - - - - - - - - - - - - - - - - (31)}$$

or

$$\beta_c = \frac{K_c^2}{B \sigma_{YS}^2} = 2\pi \text{ . - - - - - - - - - - - - - - (32)}$$

Thus when β_c is larger than 2π the resistance to rapid extension of the small through-crack should effectively arrest its spread and a stress larger than the yield stress should be required for crack propagation. On the other hand when β_c is less than 2π fast propagation begins from a small part-through starting crack and cannot be arrested by the development later of plastic yielding in the thickness direction

Normally cracks or flaws which develop into cracks occur in the rolled and welded type pressure vessels primarily in the welds or in the weld borders. The crack toughness of interest is therefore the weld or weld border toughness This can be measured by use of sheet tensile specimens as shown here on Figure 14. The slot with natural cracks at the ends is inserted either along the weld border or the weld center depending upon the measurement wanted. A number of measurements of this type have been made by Dr. Romine at the Naval Weapons Laboratory near Washington and have been published in government reports from that laboratory. K_c values were always less than those found when the starting crack was inserted in the specimen in the base metal away from the weld. For steels this difference was small when the welding and heat treating were carefully done. For Titanium alloys at a yield stress of 150,000 psi or more a weld of satisfactory toughness is a more difficult problem.

Tests of this nature have been conducted both with flush ground plate surfaces and with the extra thickness of the undressed weld present. For the latter type of specimen any weakening influence of the weld border notch must have been balanced by the strengthening or stiffening influence of the extra thickness because the supported maximum load values were essentially the same for a given crack length regardless of whether or not the weld had been flush ground. The primary advantage gained by flush grinding of welds in pressure vessels is a large increase in effectiveness and sensitivity for each of the various methods of non-destructive inspection.

We may as well note at this point that the reliability of a high strength pressure vessel for use at near yield stress level is a difficult thing to establish with certainty. The principal ingredients for success in this endeavor are meticulous inspection assisted by smooth surfaces and a degree of crack toughness sufficient to resist the spread of any small cracks which are, nevertheless, overlooked. Hydrostatic testing provides a smaller degree of assurance than one might naively expect because the vessel is weakened by the test procedure. Each loading cycle assists the spread of existing cracks and the development of others. A study of this subject is in progress at the University of Illinois based upon observations of crack growth in a high strength steel during tension-

tension-cycling. Based upon his data for M255 steel Corten* suggested that, if hydrotesting is used, the procedure should be a single loading cycle at a 10 percent overload.

Assistance from water environment to crack growth during load cycling as well as to stress rupture type of behavior has been observed in many high strength steels. For this reason moisture should be excluded from steel pressure bottles especially those expected to hold a high pressure for a long time and an oil of high dielectric constant is preferable for hydrotesting. Unfortunately for the completeness of our knowledge about influences of load cycling and stress corrosion these subjects have been studied in past years using specimens carefully prepared so that no cracks were initially present. Crack development rather than crack extension was the primary object of these studies and the information gained applied to real structures only to the degree that some correlation exists between speed of crack development and speed of crack growth. The techniques of fracture mechanics apply nicely to these subjects but most of the applying has yet to be done.

V. Sources of Crack Toughness

To assist fundamental studies of crack toughness it is clear we need measurements of crack toughness of the opening mode or plane strain type. Granting that crack toughness evaluation as now conceived must be done with relatively large starting cracks we can at least remove from the measurements the influence of plate thickness. The simplest measurement procedure to employ for this purpose uses as a test specimen a circumferentially-notched round bar in tension. The usual convention of a notch depth which makes the net section area half the gross section area is a convenient choice and a notch root radius of 0.0006", which a careful machinist can produce, is sharp enough for most metals. To insure applicability of elastic theory stress analysis the net section stress at fracture should not be larger than 1.2 times the uniaxial tensile yield stress.

Test results may be computed using the equations

$$X\left[\left(1-\frac{x^2}{2}\right)\right]^2 = 0.233\ y$$

where y is the ratio of net section stress to yield stress

---

* H. Corten, Sagamore Conference, August 1960.

$$y = \sigma_N / \sigma_{YS}$$

and

$$X = \frac{K_{Ic}}{\sigma_{YS} \sqrt{\pi D}}$$

The gross diameter of the round bar is D.

A trend in K_{Ic} values toward lower values may occur in a specific material as σ_N increases above σ_{YS}. Thus values of K_{Ic} determined in the range

$$\sigma_{YS} < \sigma_N < 1.2\ \sigma_{YS}$$

although "real" for the equivalent crack size represented may be somewhat conservative relative to larger sections containing larger cracks.

Starting crack instability develops in these tests so close to the initial edge of the notch that there is no need for ink staining to measure slow crack growth. Thus the only measurement made is maximum load and the test is convenient for use over a wide temperature range. Table II gives values of K_{Ic} and $\mathcal{G}_{Ic}$ for several materials at room temperature. Not all of these were obtained by the round notch bar procedure which was recommended above. This is also the case with the measurements shown on Figure 15. The rotor steels used had a yield strength of nearly 100,000 psi. The data came from General Electric Company tests using 6-inch thick centrally-notched discs tested by spinning them faster and faster until fracture occurred. At Westinghouse, Wessel made round notched bar tests of a material similar to that for the upper curve in a temperature range from room temperature to -380° F. His results added to the General Electric Company data, Figure 15, suggest that plane strain crack toughness is a smoothly increasing function of temperature through the entire range from -380° F to +400° F. Although there is a change in crystallinity in the appearance of the fracture facets this change also is gradual. We have as yet no evidence for any metal that the plane strain fracture toughness undergoes an abrupt upward trend at a special point in the temperature scale.

However, if the specimen dimensions and geometry permit stress relaxation parallel to the leading edge of the crack we anticipate a large and relatively abrupt increase in the mixed mode $\mathcal{G}_c$ value wil occur. The total increase in $\mathcal{G}_c$ due to this specimen dimension influence is roughly a factor of ten.

Consider next the relation of macroscopic crack toughness to the basic structure of solids. The original Griffith theory idea was to assume $\mathcal{G}_{Ic}$ equal to twice the surface energy. Gilman has suggested 2400 ergs/cm^2 would be a fair estimate of solid state surface energy for ferrite.

Table III

2γ	$(10^5$ ergs/cm$^2)$	$_{Ic}$
.05	2.5	150
	10	400

Table III shows $\mathcal{G}_{Ic}$ estimates in units of 10^5 ergs/cm^2. The entry for a guess based upon twice the solid state surface energy is about 0.05. On the right we place a value range which includes the $\mathcal{G}_{Ic}$ room temperature values for a number of tough steels. The smaller value is for tough representatives of the high strength steel class. Friedel* has discussed energy requirements for a cleavage crack moving through a forrest of dislocations. Since the crack stress field creates the dislocations their formation energy must be included. In addition dislocations introduce minute jogs or level differences in the fracture surface. He estimated these energy requirements at 50 to 200 times the surface energy. Multiplying 0.05 by 50 and 200 one obtains the range 2.5 to 10 in units of 10^5 ergs/cm^2. Granting that this is somewhat speculative it is of interest to note there still remains a substantial difference from actual measurements of $\mathcal{G}_{Ic}$. In addition to lattice slip there must be another mechanism for introduction of crack toughness. If you compare the $\mathcal{G}_{Ic}$ for dry glass and for polymethylmethacrylate in Table I you note the dry glass $\mathcal{G}_{Ic}$ is smaller by a factor of 50. Observationally the methylmethacrylate fracture surface shows parabola markings, evidence of non-planar advance fracture initiations. The glass fracture surface, on the other hand, shows none. A factor of 50 is roughly the difference which remains to be explained. From this viewpoint we can consider the toughening mechanisms for ductile metals consist in: (1) lattice slip, (2) non-coplanar fracture origins, and (3) section yielding to introduce fracture mode transition. It is this route which must be followed if we plan to calculate the fracture strength of real materials from fundamental considerations. Plastics do not possess the lattice slip mechanism and $\mathcal{G}_c$ measurements for these correspondingly small.

---

* Swampscott Conference on Fracture, 1959.

VI. A Comment on Load Transfer Balance in a Fiber Composite

Leonardo da Vinci once made a study of the strength of a supply of iron wire. Figure 16 is the drawing of his apparatus which appeared in his note book. He concluded that short lengths were stronger than long ones. Considering the quality of wire in that era a flaw probability type of size effect large enough to explain his conclusion no doubt existed. Figure 17 shows the results of measurements of specimen length effect of the da Vinci type done 400 years later at the U. S. Naval Research Laboratory using single fibers of glass. Two supplies of glass were used. In the case of the fibers used for the upper curve precautions had been taken to prevent damage in handling. For the lower curve the fibers came to us in a loose skein and contained numerous flaws. It seems a long reach from da Vinci to rocket chambers. However, those who are attempting the fiber winding type of rocket chamber construction are concerned with the length effect indicated here. If the handling of the fibers during winding introduces flaws (current procedures do little to prevent this type of damage) then there is a potentially large strength loss. But much of the intrinsic fiber strength can be recaptured if the bonding between fibers introduces sufficient load transfer so that the effective strength corresponds to very short fiber lengths. If one goes to extremes in this direction the chamber is weakened because the composite material is too brittle If the fiber bonding is relatively weak, the chamber is weakened because the strength of the effective average fiber lengths is then too small. Difficulties in maintaining a satisfactory balance removed from either of these extremes would be greatly assisted if the techniques of manufacture, coating, and winding of fibers effectively prevented introduction of flaw into the individual filaments.

Table I

Limiting Velocities of Running Cracks*

Material	Values of 0.5 c_2 Km/sec	Experimental Velocities Km/sec
Glass (Soda-lime-silica)	1.57	1.54
Glass (silica)	1.85	2.19
Cellulose Acetate	0.34	0.30
Steel (0.18 c-annealed)	1.58	1.50
Columbia Resin (CR-39)	0.47	0.55

$$\mu = \rho c_2^2 = \frac{E}{2(1+\nu)}$$

E = Young's Modulus ν = Poisson's ratio

ρ = density

NOTE:

Glass data -- H. Rawson, Society of Glass Tech. 36, 173, (1952)

Cellulose acetate data -- H. L. Smith and W. J. Ferguson,
Naval Research Laboratory
Progress Report, April 1950

Steel data -- OSRD Report No. 6452, Jan. 1946

CR-39 data -- Wells and Post,
NRL Report No. 4935, April 23, 1957

---

* Table prepared by H. L. Smith

Table II

Selected $\mathcal{G}_{Ic}$ Values
(Room Temperature)

	Tensile Yield Strength (Ksi)	$\mathcal{G}_{Ic}$ (Lbs/in)
Glass, lantern slide (2% RH)	100	0.08
Polyesters (cast plates)	15	1.0
Polymethylmethacrylate (cast plates)	10	4.0
7075-T6 aluminum	72	145
2024-T3 aluminum	50	800
Rotor steel (low quality)	95	120
Gun steel (high strength)	207	230
Hot die steel (H-11)	225	65
Hot die steel (H-11)	245	35

References

1. H. M. Westergaard, "Bearing Pressures and Cracks", Trans. ASME, Vol. 61, 1939, p. A-49.

2. A. A. Griffith, "The Phenomenon of Rupture and Flow in Solids", Phil. Trans. Roy. Soc. London, Series A, Vol. 221, 1920, p. 163.

3. G. R. Irwin, "Fracture Mechanics in Structural Mechanics, Pergamon Press, 1960.

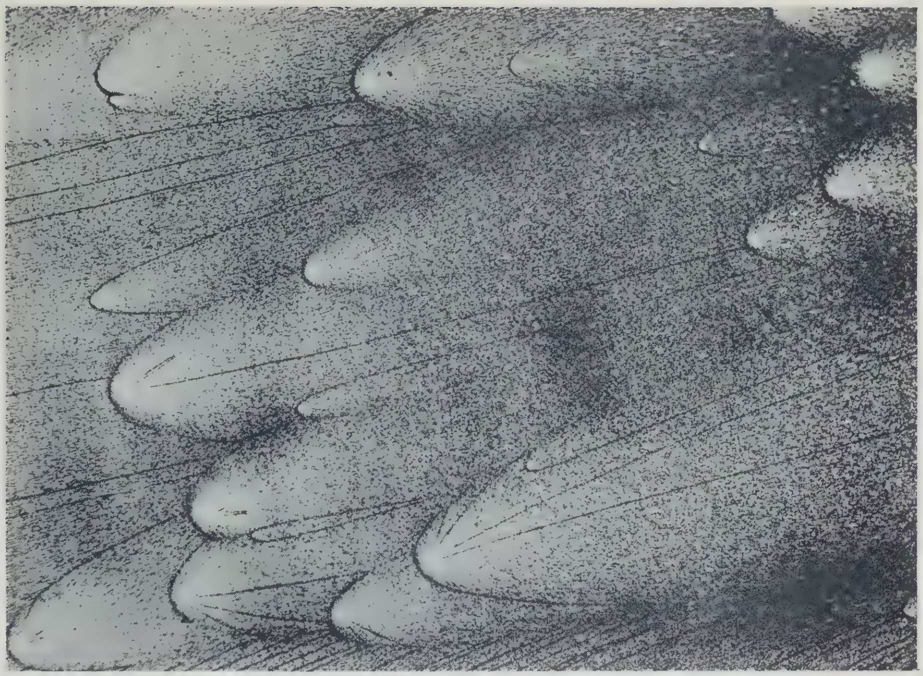

Fig. 1 Parabola Markings on Plexiglas

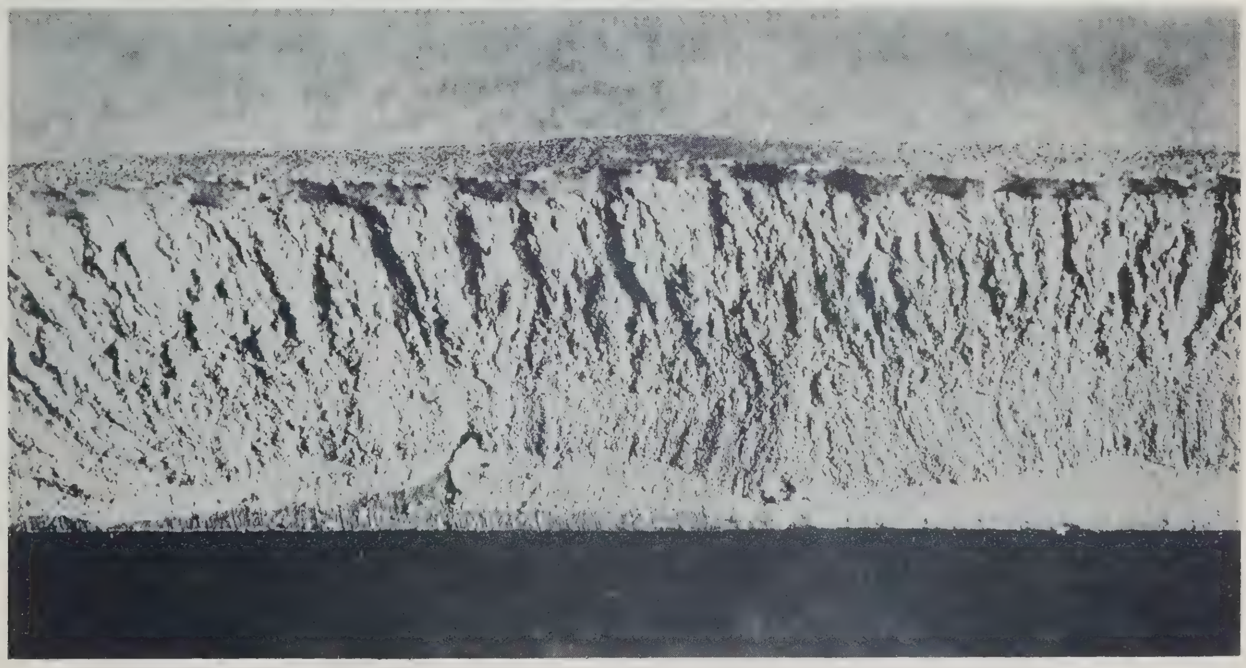

Fig. 2 Fracture Origin Showing Arrest Lines

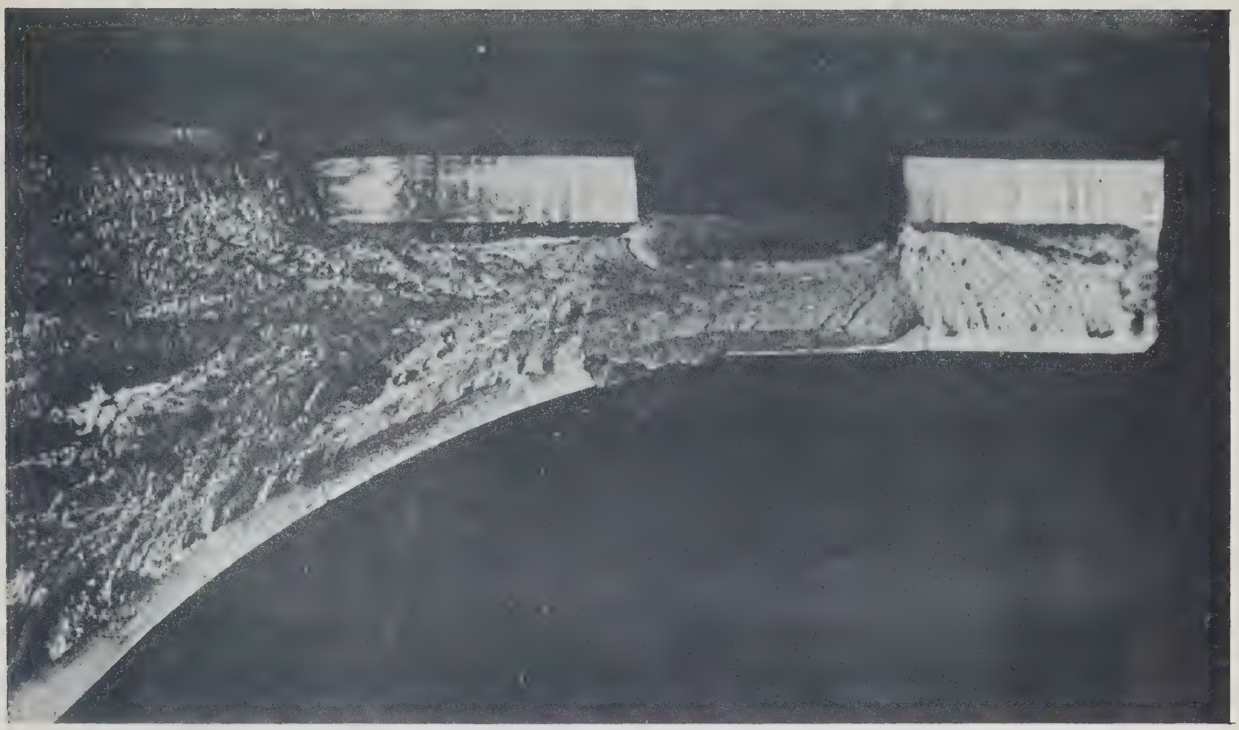

Fig. 3 Fracture Originating at the Intersection of a Keyway

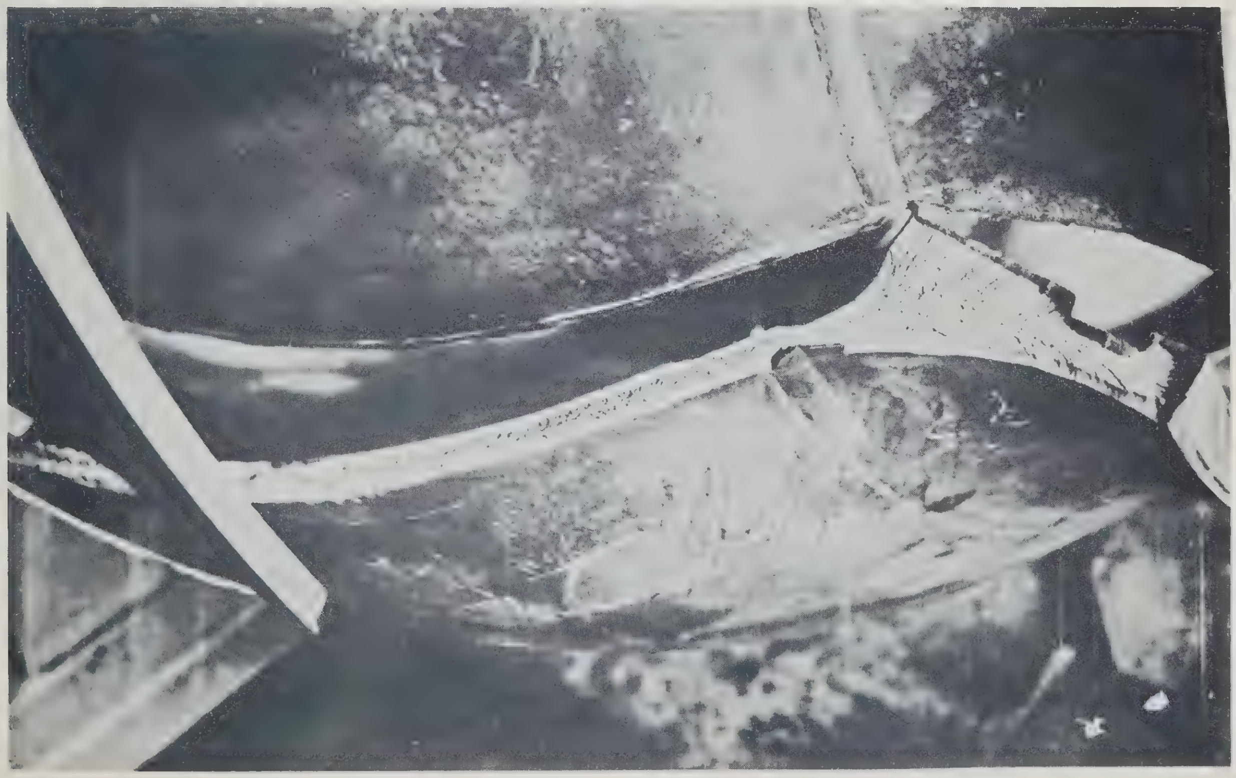

Fig. 4 Fracture Originating Through a Similar Section but Ending at Keyway

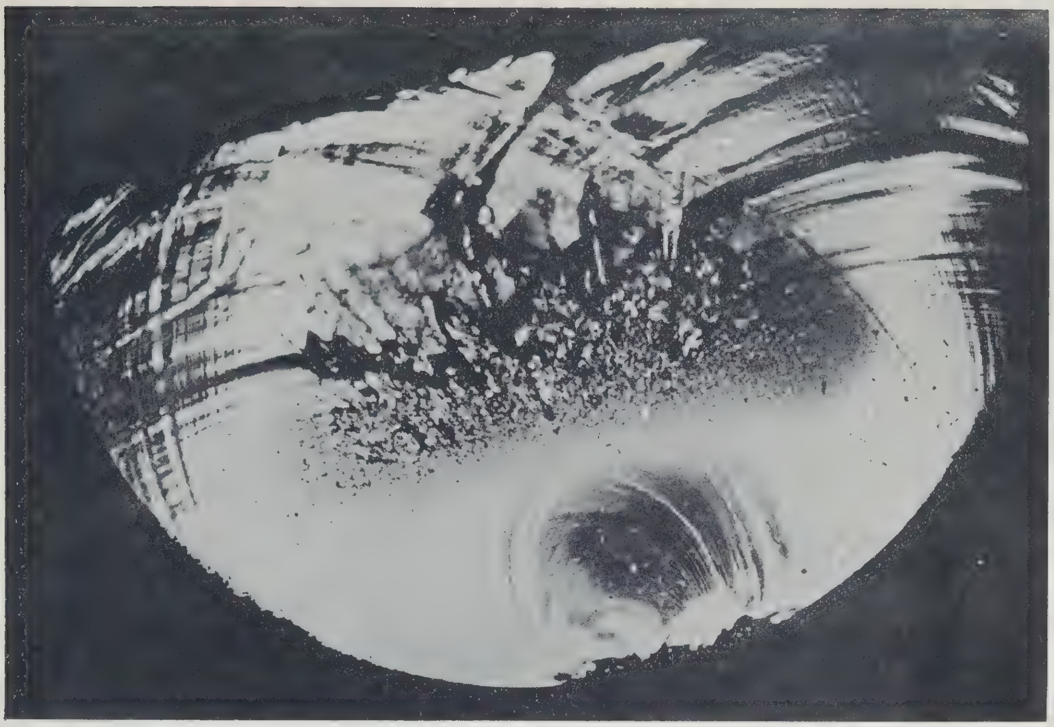

Fig. 4-1 Glass Rod Fracture Showing Wollner Lines and Hackle

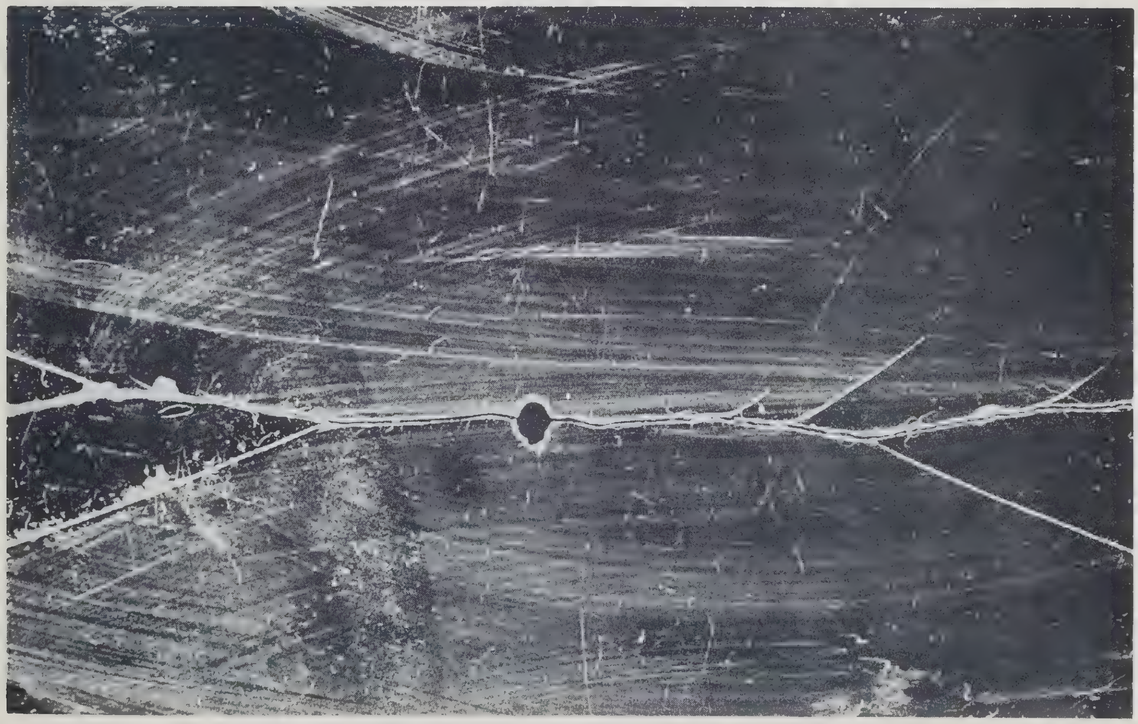

Fig. 4-2 Fracture of a Plexiglas Sheet in Tension from a Cal. 22 Bullet Perforation Shows Multiple Branching

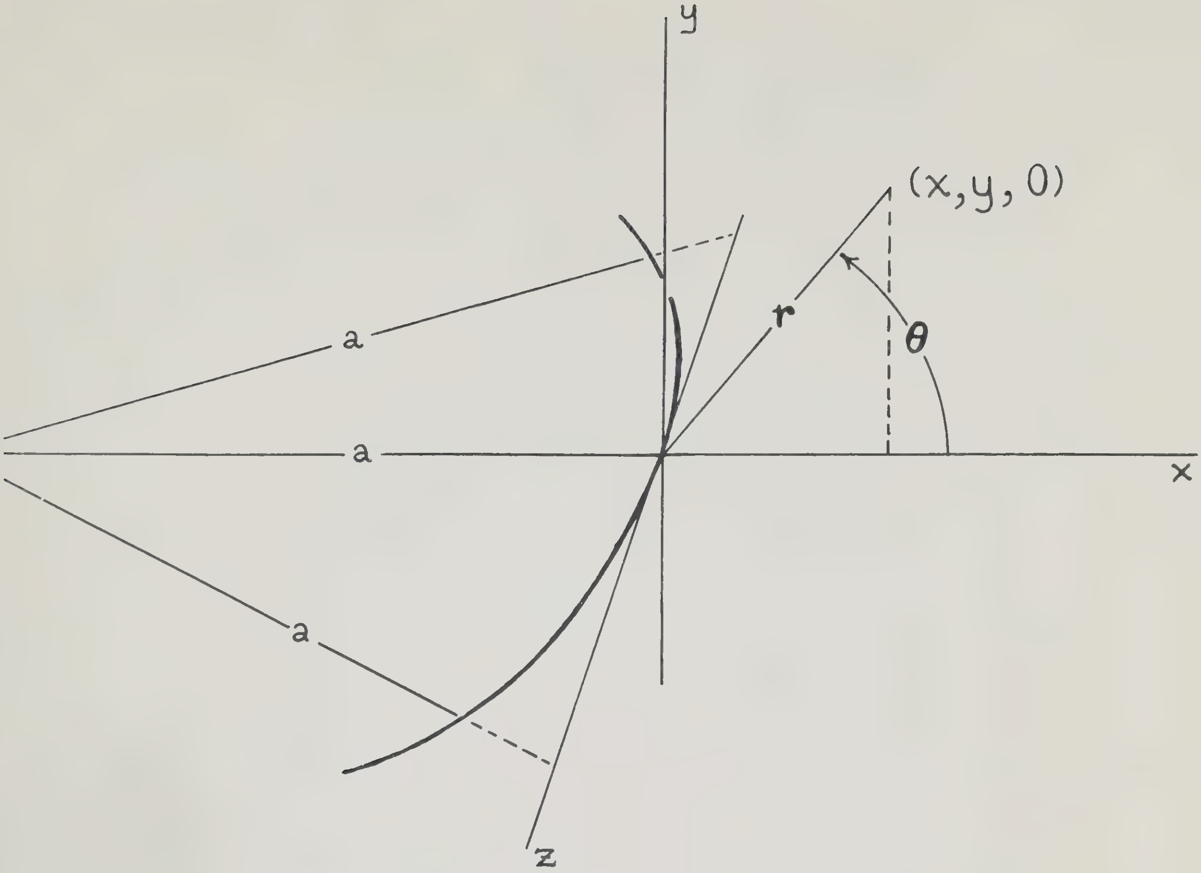

Fig. 5 Rectangular Coordinates, x, y, z, and Polar Coordinates, r, θ, at the Edge of a Penny-shaped Interior Crack

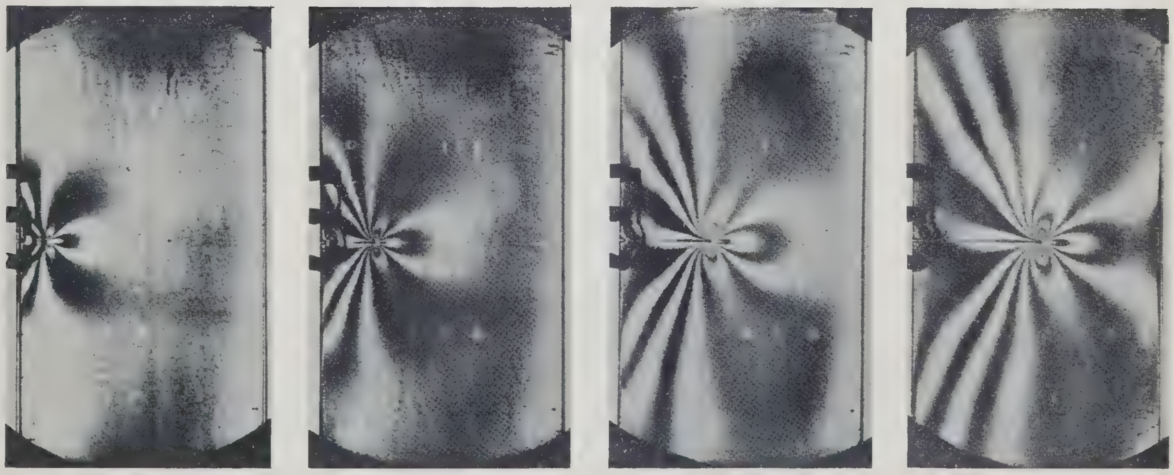

Fig. 6 Isochromatic Fringes - 4 Micro-flash Views of the Same Crack Traversing a Sheet of Columbia Resin (Wells and Post)

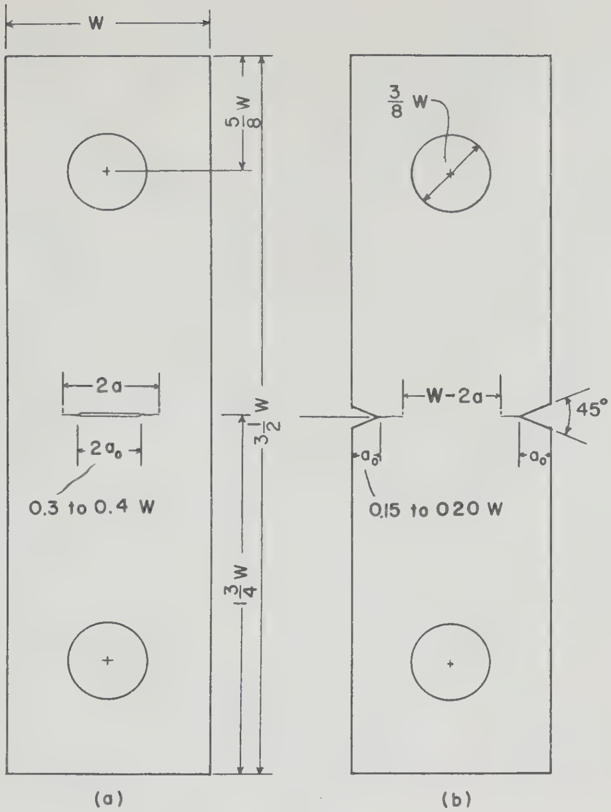

Fig. 7 Central-notch and Edge-notch Sheet Tensile Specimens

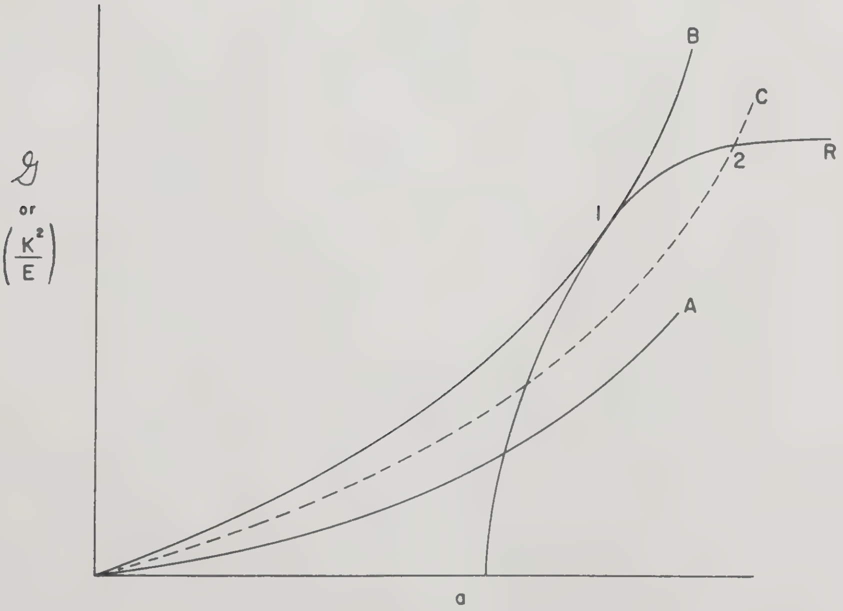

Fig. 8 Schematic Curves Showing Growth of Resistance to Crack Extension, Curve R, and Three $\mathcal{G}$ Versus a Curves (Each for a Different Fixed Tensile Load, σ)

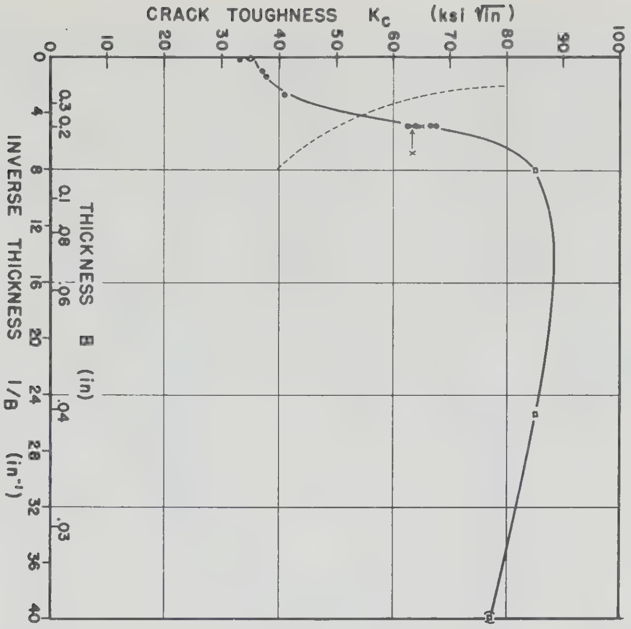

Fig. 9 Width Effect in Sheets of 7075-T6 Aluminum. K_{co} Values Were Computed Using no Plastic Strain Correction. Tension was Transverse to the Rolling Direction

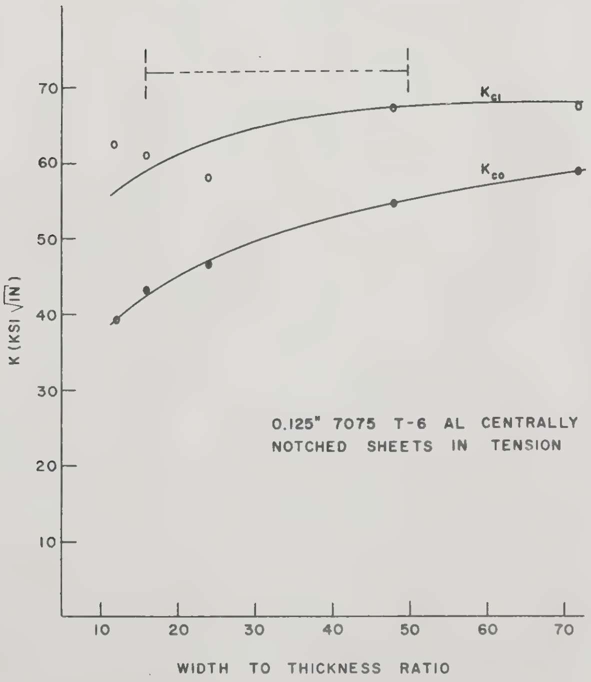

Fig. 10 K_c Versus Reciprocal Plate Thickness 1/B for 7075-T6 Aluminum. Tension was Parallel to the Rolling Direction

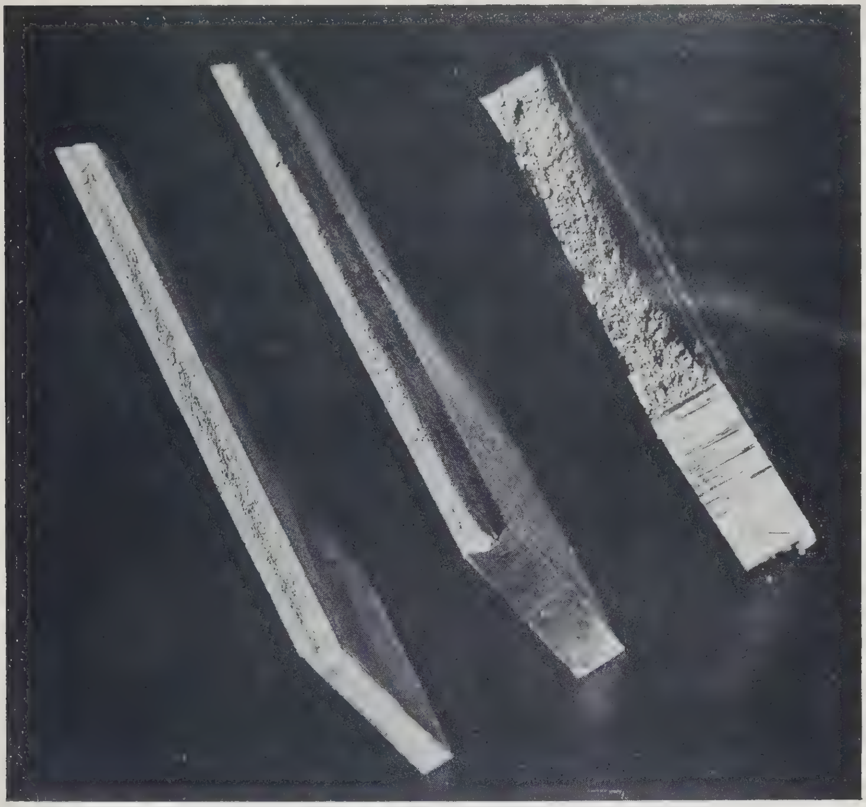

Fig. 11 Fracture Appearance for 1/4", 3/16" and 1/8" Plates of 7075-T6 Aluminum

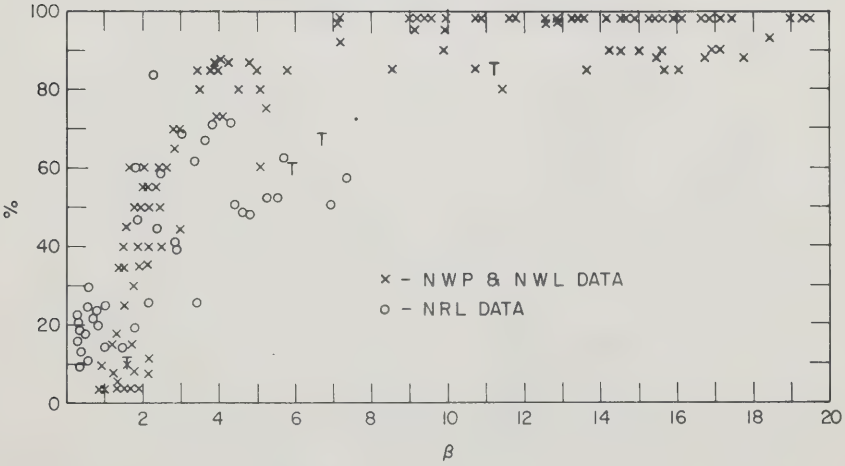

Fig. 12 Percent Shear Lip as a Function of β_c for a Variety of Heat Treatments of Various High-Strength Steels (X, O) and Titanium Alloys (T). Sheet Thicknesses Ranged from 0.07 in. to 0.22 in. and all Tests Were at Room Temperature

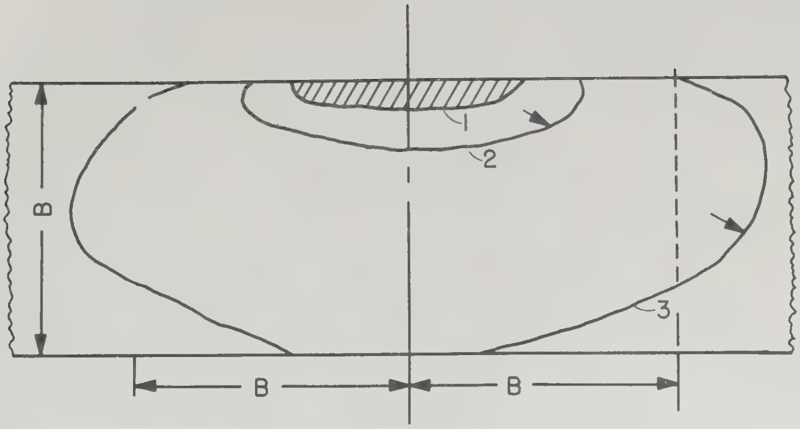

Fig. 13 Spreading of Part-Through Crack

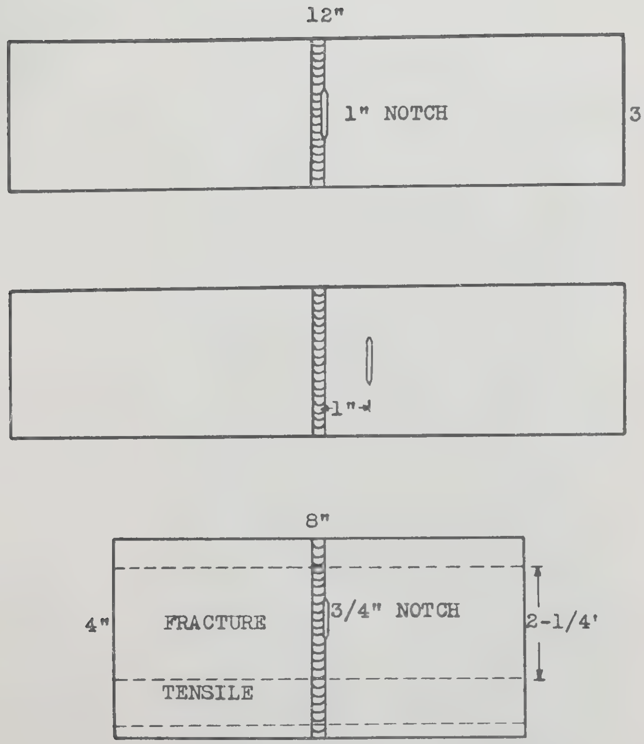

Fig. 14 Typical Test Specimens for Measurement of Weld Border and Base Metal Crack Toughness

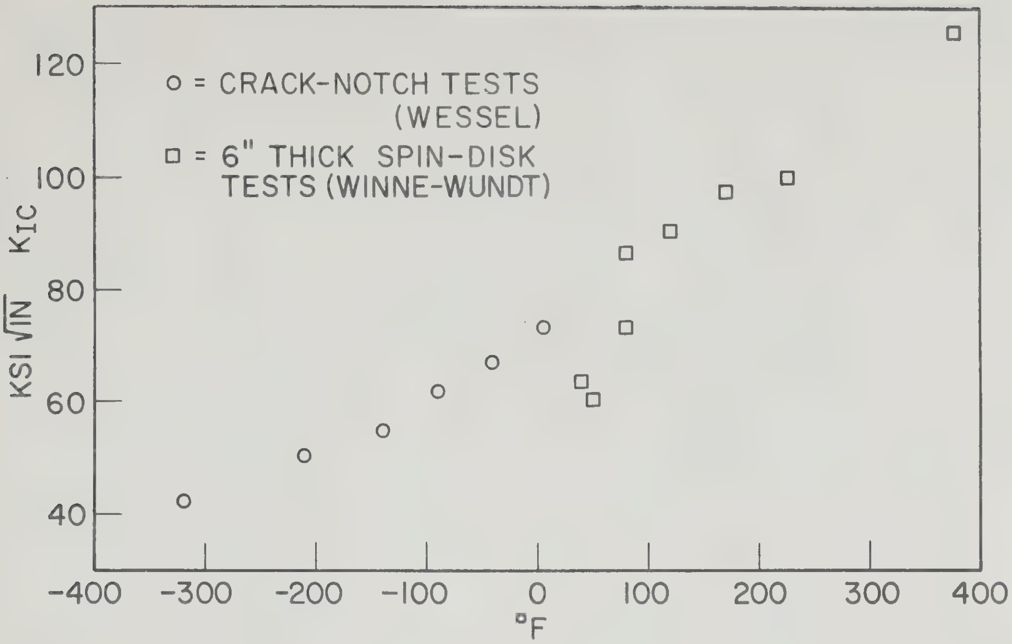

Fig. 15 K_{Ic} Values from Crack-Notch Tensile Tests by Wessel on Specimens from a Rotor Steel Forging are Shown in the Range-320°F Through 0°F KIc Values Calculated from Centrally Notched Spin Disk Tests Reported by Winne and Wundt for a Similar Rotor Forging are Shown in the Range 0°F to 400°F

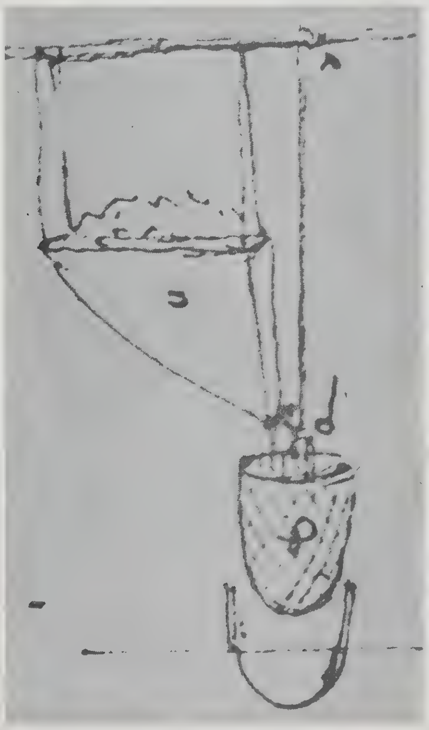

Fig. 16 Sketch by Leonardo da Vinci of his Apparatus for Testing Iron Wire

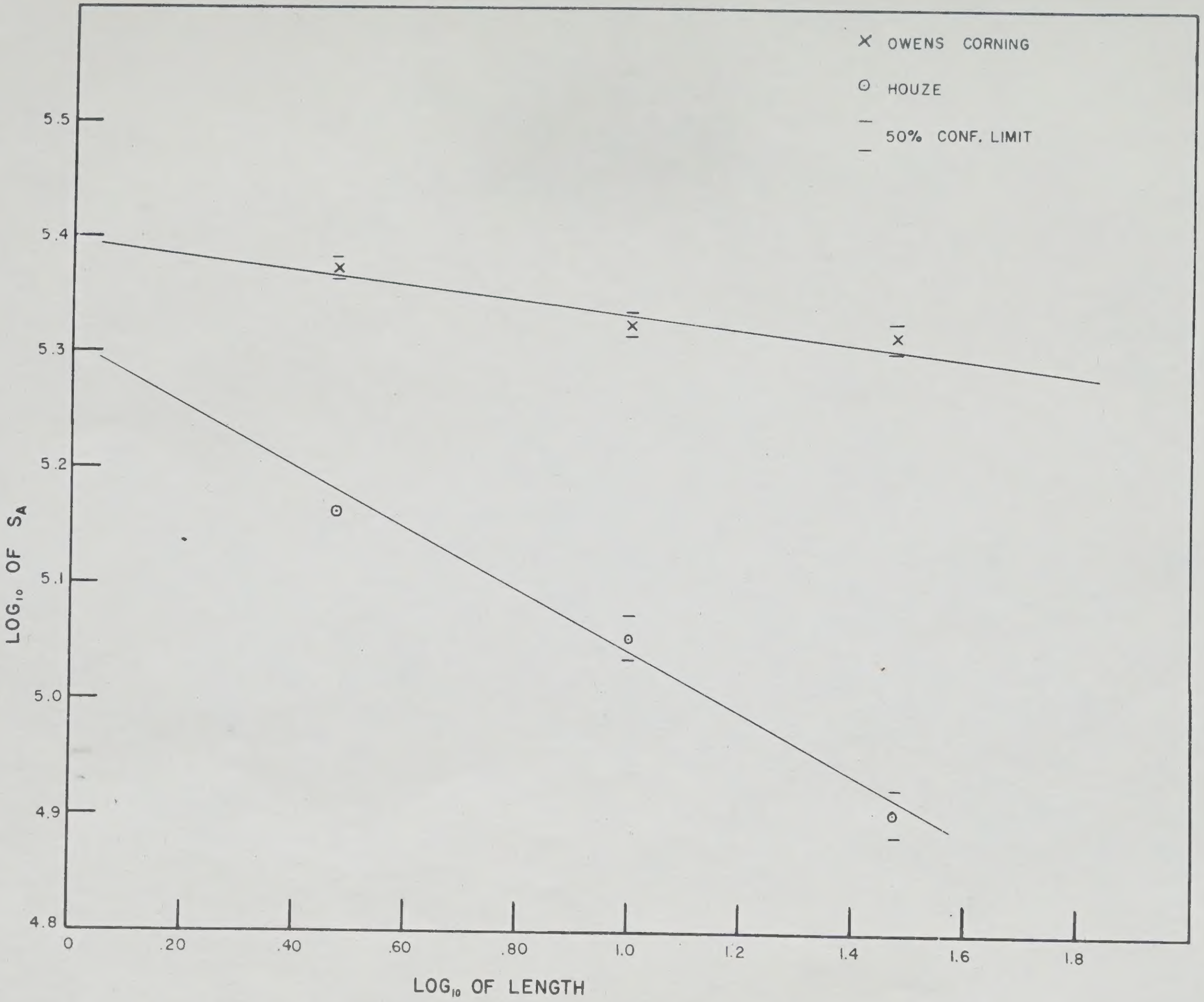

Fig. 17 Logarithm of Average Tensile Strength (psi) as a Function of Logarithm of Specimen Length (cm) for Carefully Protected Glass Fibers (x) and Fibers Damaged by Rough Handling (o)

LIST OF RECENT REPORTS

Number	Title and Author	Date
189	"A Resolved Shearing Stress Energy Theory of Failure by Slip of a Polycriptalline Metal with Face-Centered Cubic Lattice Crystals", by James O. Smith	May, 1961
190	"Stresses Due to Rotating Inertia Force in a Hollow Circular Cylinder", by Howard B. Wilson	May, 1961
191	"Second Student Symposium on Engineering Mechanics"	June, 1961
192	"Inelastic Buckling of Columns With Elastically Restrained Ends", by William H. Collins and O. M. Sidebottom	June, 1961
193	"Effect of Loading Sequence on Cumulative Fatigue Damage of 7075-T6 Aluminum Alloy", by R. Spitzer and H. T. Corten	June, 1961
194	"Shear Strength of Two-Span Continuous Reinforced Concrete Beams With Multiple Point Loading", by R. H. Bryant, A. C. Bianchini, J. J. Rodriquez and C. E. Kesler	July, 1961
195	"Analysis of Missile Launchers - Part O, Phase O. Multi - degree of Freedom Models", by G. A Wempner and S. K. Lee	July, 1961
196	"Creep of Thick-Walled Cylinders Under Internal Pressure and Axial Load", by J. W. Schweiker and O. M. Sidebottom	July, 1961
197	Response of a Linear Two Degree of Freedom System to Multiple Excitations", by J. A. Kasuba	August, 1961
198	"Creep Torsion of Non-Circular Prismatic Bars", by John L. Gubser and O. M. Sidebottom	August, 1961
199	"Study of Nonlinear Vibration Isolation Systems - Part II - One Degree of Freedom, -Transient Excitations", by Will J. Worley and Frank H. Brittain	August, 1961
200	"Bond and Anchorage Characteristics of Welded Wire Fabric in Concrete", by D. W. Pfeifer, A.C. Bianchini and C. E. Kesler	September, 1961
201	"Inelastic Design of Load Carrying Members. Part V. Theoretical and Experimental Creep Analyses of Beam-Columns" by D. L. Dewhirst and O. M. Sidebottom	October, 1961

UNIVERSITY OF ILLINOIS-URBANA
620.1123IR9F C001
FRACTURING AND FRACTURE MECHANICS$URBANA
3 0112 007752261

PUBLIC SERVICE
RESEARCH TAM TEACHING
UNIVERSITY OF ILLINOIS